Korean J Physiol Pharmacol 2024;28(4):335-344
https://doi.org/10.4196/kjpp.2024.28.4.335

KJPP

Original Article

# The NADPH oxidase inhibitor diphenyleneiodonium suppresses $Ca^{2+}$ signaling and contraction in rat cardiac myocytes

Qui Anh Le[1,#], Tran Nguyet Trinh[1,#], Phuong Kim Luong[1], Vu Thi Van Anh[1], Ha Nam Tran[1], Joon-Chul Kim[1,2], and Sun-Hee Woo[1,*]

[1]College of Pharmacy, Chungnam National University, Daejeon 34134, [2]Nexel Co. Ltd., Seoul 07802, Korea

**ARTICLE INFO**

**Received** April 8, 2024
**Revised** April 14, 2024
**Accepted** April 15, 2024

***Correspondence**
Sun-Hee Woo
E-mail: shwoo@cnu.ac.kr

**Key Words**
Cardiac myocytes
$Ca^{2+}$ release
Contraction
Diphenyleneiodonium
L-type $Ca^{2+}$ current

#These authors contributed equally to this work.

**ABSTRACT** Diphenyleneiodonium (DPI) has been widely used as an inhibitor of NADPH oxidase (Nox) to discover its function in cardiac myocytes under various stimuli. However, the effects of DPI itself on $Ca^{2+}$ signaling and contraction in cardiac myocytes under control conditions have not been understood. We investigated the effects of DPI on contraction and $Ca^{2+}$ signaling and their underlying mechanisms using video edge detection, confocal imaging, and whole-cell patch clamp technique in isolated rat cardiac myocytes. Application of DPI suppressed cell shortenings in a concentration-dependent manner ($IC_{50}$ of ≅0.17 μM) with a maximal inhibition of ~70% at ~100 μM. DPI decreased the magnitude of $Ca^{2+}$ transient and sarcoplasmic reticulum $Ca^{2+}$ content by 20%–30% at 3 μM that is usually used to remove the Nox activity, with no effect on fractional release. There was no significant change in the half-decay time of $Ca^{2+}$ transients by DPI. The L-type $Ca^{2+}$ current ($I_{Ca}$) was decreased concentration-dependently by DPI ($IC_{50}$ of ≅40.3 μM) with ≅13.1%-inhibition at 3 μM. The frequency of $Ca^{2+}$ sparks was reduced by 3 μM DPI (by ~25%), which was resistant to a brief removal of external $Ca^{2+}$ and $Na^{+}$. Mitochondrial superoxide level was reduced by DPI at 3–100 μM. Our data suggest that DPI may suppress L-type $Ca^{2+}$ channel and RyR, thereby attenuating $Ca^{2+}$-induced $Ca^{2+}$ release and contractility in cardiac myocytes, and that such DPI effects may be related to mitochondrial metabolic suppression.

## INTRODUCTION

The contraction of mammalian cardiac myocytes is controlled by a transient increase in cytosolic $Ca^{2+}$ concentration *via* sarcoplasmic reticulum (SR) $Ca^{2+}$ release upon depolarization. Membrane depolarization induces $Ca^{2+}$ influx through the L-type $Ca^{2+}$ channels, which, in turn, triggers the release of large amounts of $Ca^{2+}$ from the SR into the cytosol [1-4]. Confocal $Ca^{2+}$ imaging of cardiac myocytes has revealed local $Ca^{2+}$ releases through ryanodine receptors (RyRs) ("$Ca^{2+}$ sparks") triggered either spontaneously or by L-type $Ca^{2+}$ current ($I_{Ca}$) [5-7]. $Ca^{2+}$ sparks are thought to be elementary $Ca^{2+}$ release events that underlie global $Ca^{2+}$ release upon depolarization in cardiac myocytes [5-9].

Reactive oxygen species (ROS) oxidize macromolecules including RyRs and are extensively involved in physiological and pathological processes in cardiac muscle [10-13]. The NADPH oxidase (Nox) is one of the major sources for superoxide anion ($O_2^{\cdot-}$) in cardiac myocytes under various external stimuli including mechanical stresses and plays a central role in $Ca^{2+}$ mobilization *via* RyRs [14-19]. Diphenyleneiodonium (DPI) has been known as a representative Nox inhibitor [20] and often used for this purpose [16-18,21]. However, DPI has exerted diverse inhibitory effects in



**Author contributions:** Q.A.L. and T.N.T. wrote original draft and performed the experiments. P.K.L., V.T.V.A., H.N.T., and J.C.K. performed the experiments and analyzed the data. S.H.W. designed and supervised this study and did editing. All authors read and approved the final manuscript.

different mammalian cell types including mitochondrial Complex I [22-25], cholinesterase [26], nitrogen oxide synthase (NOS) [27,28], and xanthin oxidase [29]. These reports raise concerns about interpretation of data obtained using DPI and suggest an involvement of ubiquitous signaling molecule in the side effects by DPI.

We have previously found that DPI, at the concentrations used to eliminate the Nox activity (~3 μM), significantly reduces the occurrence of spontaneous $Ca^{2+}$ sparks in rat ventricular myocytes under control conditions, although the specific inhibitor of Nox 2 (*e.g.*, gp91-ds) did not alter the occurrence of $Ca^{2+}$ sparks [18]. Therefore, we hypothesized that DPI may affect global $Ca^{2+}$ signals and contraction independently of its action on Nox in cardiac myocytes. To test this hypothesis, we examined the effects of DPI on contraction, global $Ca^{2+}$ signaling and $I_{Ca}$, and cellular mechanism for the effects in isolated rat ventricular myocytes using a video edge detection, confocal imaging, and whole-cell patch clamp technique. Here we describe inhibition of excitation-contraction coupling by DPI in ventricular myocytes.

# METHODS

## Cell isolation

Cardiac myocytes were isolated from male Sprague-Dawley rats (200–300 g) as previously described [30]. The experiments were performed in accordance with the principles for the care and use of experimental animals published by the Korean Food and Drug Administration. The surgical method was approved by the Animal Care and Use Committees of the Chungnam National University (CNU-00992). Briefly, after rats were anesthetized with sodium pentobarbital (150 mg/kg, intraperitoneal injection), the hearts were taken out with thoracotomy. Then, aorta was tied onto the cannular of Langendorff apparatus for retrograde perfusion at 7 ml/min through the aorta (at 36.5°C). The heart was perfused first with $Ca^{2+}$-free Tyrode's solution composed of (in mM) 137 NaCl, 5.4 KCl, 10 HEPES, 1 $MgCl_2$, and 10 glucose (pH 7.3) for 3 min, and then with $Ca^{2+}$-free Tyrode's solution containing collagenase (1.4 mg/ml, type A; EC 3.4.24.3; Sigma-Aldrich) and protease (0.14 mg/ml, type XIV; EC 3.4.24.31; Sigma-Aldrich) for about 12 min. Then, the heart was perfused with Tyrode's solution containing 0.2 mM $Ca^{2+}$ for further 5 min. The digested heart was then cut and chopped into pieces for further dissociation of myocytes.

## Measurement of cell shortenings

Ventricular myocytes attached at the bottom of experimental chamber were continuously superfused with normal Tyrode's solutions (pH = 7.4) containing 2 mM $Ca^{2+}$ and field-stimulated at 1 Hz with two paralleled Pt wires connected to an electrical stimulator (D-7806; Hugo Sachs) at room temperature. Cell shortenings were detected with a video edge detector (Model VED-105; Crescent Electronics) connected to a CCD camera (LCL902C; Till Photonics) and video monitor (ViewFinder III, Polychrome V system; Till Photonics) as previously reported [30]. Changes of cell length were monitored using A/D converter (Digidata 1322A; Molecular Devices) connected to a PC software pClamp (9.0; Molecular Devices) and analyzed with Clampfit 9.0 (Molecular Devices) and Origin software (8.0; OriginLab Corporation).

## Two-dimensional (2-D) confocal $Ca^{2+}$ imaging and image analysis

To detect cytosolic $Ca^{2+}$ ventricular myocytes were loaded with 3 μM fluo-4 acetoxymethyl (AM) ester (Thermo Fisher Scientific) for 30 min. The dye-loaded cells were continuously superfused with 2-mM $Ca^{2+}$-containing normal Tyrode's solutions (pH 7.4; see above). Dyes were excited at 488 nm using Ar ion laser, and fluorescence emission at > 510 nm was detected. Cytosolic $Ca^{2+}$ fluorescence signals were recorded in 2-D images using a laser scanning confocal imaging system (A1; Nikon) attached to an inverted microscope (Eclipse Ti; Nikon) fitted with a ×60 oil immersion objective lens (Plan Apo, Numerical Aperture 1.4; Nikon) [30]. Acquisition and analysis of images were performed using a workstation software (NIS Elements AR, v3.2; Nikon).

To record global $Ca^{2+}$ transients, images were captured at 120 Hz in the field-stimulated (1 Hz) cells with two paralleled Pt wires connected to an electrical stimulator (D-7806; Hugo Sachs). The average diastolic fluorescence intensity ($F_0$) was measured from several frames captured before the upstroke of $Ca^{2+}$ transient. The time-courses of $Ca^{2+}$ transients were evaluated as the average fluorescence of each area normalized relative to the $F_0$ ($F/F_0$) [30]. To measure $Ca^{2+}$ spark frequency, the whole-cell images were recorded at 30 Hz. Recording of spontaneous sparks was preceded by a series of electrical pulses at 1 Hz to maintain the SR $Ca^{2+}$ content. $Ca^{2+}$ sparks were identified by a computerized algorithm in the "RealTimeMicroscopy" PC program (own written in C++) as previously described [18]. In order to calculate the frequency of sparks ([total number of sparks]/[$10^3$ $\mu m^2 \cdot s$]), whole-cell areas were measured using the NIS Elements AR software (v3.2; Nikon).

## Measurements of $I_{Ca}$

$I_{Ca}$ was recorded using the whole cell configuration of the patch-clamp technique using an EPC7 amplifier (HEKA) as previously described [31]. The patch pipettes were made of glass capillaries (Kimble Glass) to have resistance of 2–3 MΩ. Internal solution contained (in mM) 110 CsCl, 20 TEA-Cl, 20 HEPES, 5 MgATP, and 15 EGTA, with the pH adjusted to 7.2 (with CsOH). Outward $K^+$ currents were suppressed by internal $Cs^+$ and $TEA^+$, and inward rectifier $K^+$ current was suppressed by replacing ex-

ternal $K^+$ with $Cs^+$. $Na^+$ current was inactivated by holding the membrane potential at −40 mV. Recording of $I_{Ca}$ was carried out ~8 min after a rupture of the membrane with the patch pipette, when the rundown of $Ca^{2+}$ channels were slowed and stabilized. Using pCLAMP (9.0; Molecular Devices) combined with an analog-to-digital converter (Digidata 1322; Molecular Devices) we applied voltage commands and acquired current data. The series resistance was ~2 times the electrode resistance and was compensated through the amplifier. The current signals were filtered with low pass filter at 1 kHz and digitized at 10 kHz. The current data were analyzed using Clampfit (9.0; Molecular Devices). The time constant (τ) of inactivation of $I_{Ca}$ was obtained with single exponential curve fitting using the equation:

$$y = (A_i - A_f) \cdot \exp(-t/\tau) + A_f,$$

where $A_i$ and $A_f$ are the initial ($t$ = 0) and final ($t$ = infinity) values of the parameter, and τ is a time constant of exponential decay. Curve fitting was performed using OriginPro 8 SR0 software (OriginLab Corporation). The percent suppressions of $I_{Ca}$ by various interventions were evaluated after a gradual decrease in $I_{Ca}$ by rundown was subtracted from the raw current [31].

## Measurements of mitochondrial ROS

To measure mitochondrial $O_2^{\cdot-}$, cells were loaded with MitoSOX Red (10 μM; Thermo Fisher Scientific) for 30 min. Fluorescence signal was imaged using the same confocal system at 5-s intervals [18]. MitoSOX Red was excited with light at 514 nm while measuring the emitted light collected at 570–620 nm. To prevent artefactual signal due to light exposure low imaging speed was used. The time course of the MitoSOX fluorescence was evaluated as the average fluorescence of each area normalized to control fluorescence detected prior to DPI exposure ($F_0$).

## Solutions and reagents

DPI was purchased from Sigma-Aldrich. DPI was diluted in Tyrode's solution for testing (dimethylsulfoxide [DMSO] ≤ 0.08% (v/v), *e.g.*, 0.01% DMSO at 3-μM DPI solutions). Same concentrations of DMSO were added to external solutions without or with DPI. The drug solutions were applied to the cells by superfusion using custom-made solution switching apparatus except the experiments using caffeine, and zero $Na^+$ and zero $Ca^{2+}$ external solutions. To make zero $Na^+$ and zero $Ca^{2+}$ external solutions, 137 mM $Na^+$ and 2 mM $Ca^{2+}$ were removed with adding 1 mM EGTA and 137 mM LiCl. Zero $Na^+$ and zero $Ca^{2+}$ external solutions and 10 mM caffeine-containing external solutions were rapidly applied using own made puffing device. All the experiments were performed at room temperature (22°C–25°C).

## Statistics

The numerical results are presented as means ± standard error of the mean. *n* indicates number of cells used. The Student's t-tests were used for statistical comparisons depending on the experiments. Differences were considered to be significant to a level of $p < 0.05$.

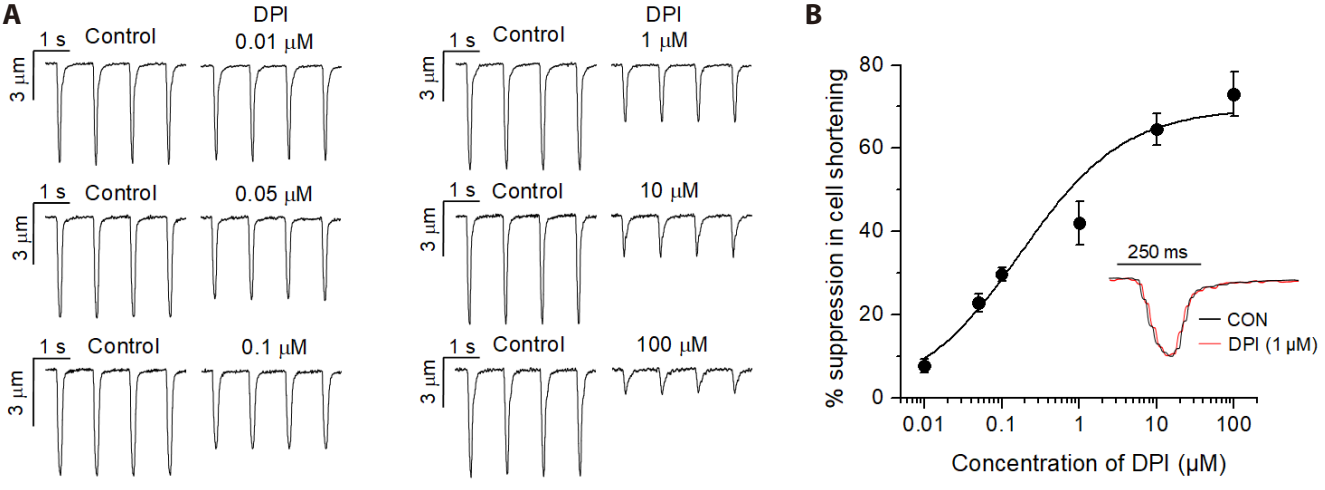


**Fig. 1. Negative inotropy induced by diphenyleneiodonium (DPI) in rat ventricular myocytes.** (A) Representative contraction traces recorded immediately before ("Control") and after the exposure to different concentrations of DPI in field-stimulated rat ventricular myocytes at 1 Hz. The traces were selected when a maximal decrease in cell shortening by DPI was observed. (B) Concentration-dependent decrease in cell shortenings (% suppression) by the extracellular application of DPI; 0.01 μM, $n$ = 3, $p > 0.05$; 0.05 μM, $n$ = 4, $p < 0.01$; 0.1 μM, $n$ = 4, $p < 0.01$; 1 μM, $n$ = 6, $p < 0.001$; 10 μM, $n$ = 6, $p < 0.0001$; 10 μM, $n$ = 4, $p < 0.001$. Paired t-test was used. The sigmoidal curve represents the fit of the Hill equation.

# RESULTS

## Effects of DPI on contraction in rat ventricular myocytes

Fig. 1 shows the effects of different concentrations of DPI on cell shortenings in rat ventricular myocytes stimulated at 1 Hz. Cell shortenings were reduced by the application of DPI in a concentration-dependent manner (Fig. 1): % inhibition: 7.65 ± 1.61, 22.8 ± 2.19, 29.7 ± 1.63, 42.0 ± 5.28, 64.5 ± 3.80, and 73.0 ± 5.30 at the concentrations of 0.01, 0.05, 0.1, 1, 10 and 100 μM, respectively. Curve fitting for the concentration-response plot using Hill equation showed 50%-inhibition in contraction by DPI at ≅0.17 μM with maximal inhibition of 69.5 ± 6.34% at 100 μM (Fig. 1B). DPI did not significantly alter the time-to-peak of contraction, the time-to-relaxation and the rates of contraction and relaxation (Table 1 and Fig. 1B, inset).

**Table 1. Effects of DPI on the kinetics of cell contraction and relaxation**

| | Control | DPI (1 μM) |
|---|---|---|
| Time-to-peak (ms) | 82.1 ± 6.24 | 89.3 ± 11.2 |
| Time-to-relaxation (ms) | 183 ± 10.3 | 206 ± 19.8 |
| Rate of contraction (μm/s) | 69.4 ± 8.61 | 66.8 ± 9.23 |
| Rate of relaxation ([μm/s) | 13.8 ± 2.52 | 12.6 ± 2.76 |

Data represents mean ± SEM. Stable six cells were analyzed. DPI, diphenyleneiodonium.

## Attenuation of global $Ca^{2+}$ signaling by DPI

To determine the cellular mechanism underlying the negative inotropy in the presence of DPI, we examined the effects of DPI on global $Ca^{2+}$ signaling in these myocytes. Fig. 2 represents a series of $Ca^{2+}$ transients measured from a field-stimulated ventricular myocyte, followed by a $Ca^{2+}$ signal induced by the treatment of 10 mM caffeine in resting condition, before and after the application of DPI (3 μM). We tested DPI at the concentration of 3 μM, which showed submaximal effects on cell shortening and was used to examine the role of Nox in cardiac myocytes [16,18]. The results showed that the systolic $Ca^{2+}$ levels and the magnitudes of $Ca^{2+}$ transients were significantly decreased by DPI (% of control: systolic $Ca^{2+}$, 93.1 ± 1.9, $p < 0.01$; magnitude of $Ca^{2+}$ transient, 80.1 ± 2.7, $p < 0.0001$; $n = 15$; Fig. 2A, B). Diastolic $Ca^{2+}$ levels were not

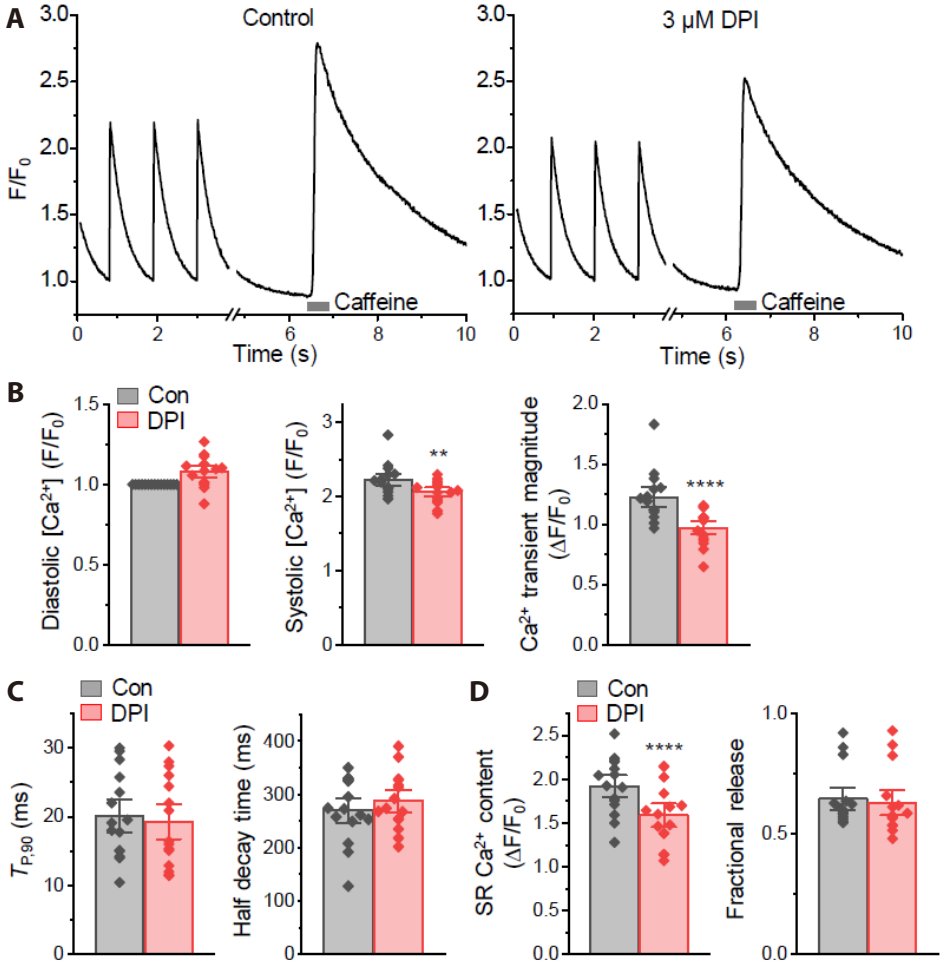


**Fig. 2. Alterations of global $Ca^{2+}$ signaling in the presence of diphenyleneiodonium (DPI).** (A) $Ca^{2+}$ transients measured in a representative ventricle cell followed by caffeine (10 mM)-induced $Ca^{2+}$ signals in the absence and presence of 3 μM DPI. (B, C) Summary of mean values of the diastolic and systolic $Ca^{2+}$ levels, and in the magnitude, time-to-90%-peak ($T_{P,90}$) and half decay time of $Ca^{2+}$ transient in the absence (Con) and presence of DPI (3 μM) ($n = 15$). ****$p < 0.0001$, **$p < 0.01$ *vs.* Con (Paired t-test). (D) Comparison of magnitudes of the caffeine-induced $Ca^{2+}$ transients and fractional release measured before (Control) and after application of DPI (3 μM) ($n = 15$). ****$p < 0.0001$ *vs.* Con (Paired t-test).

significantly altered by DPI (% of control: 108 ± 2.4, $p > 0.05$, $n = 15$; Fig. 2A, B). The kinetics of release and decay of $Ca^{2+}$ during depolarization, estimated as the time-to-90%-peak ($T_{P,90}$) and the half-decay time ($D_{1/2}$), was not significantly altered by DPI (Fig. 2C; % of control: $T_{P,90}$, 96.4 ± 6.4, $p > 0.05$; $D_{1/2}$, 103 ± 3.5, $p > 0.05$, $n = 15$).

The SR $Ca^{2+}$ loading status, evaluated by the magnitude of caffeine-induced $Ca^{2+}$ transients (Fig. 1A), was significantly reduced by the exposure to DPI (Fig. 2D; % of control in 3 μM DPI: 82.6 ± 2.8%, $p < 0.001$, $n = 15$). Fractional release, the ratio of depolarization-induced $Ca^{2+}$ release to caffeine-induced $Ca^{2+}$ release, was not affected by DPI (Fig. 2D; % of control in 3 μM DPI: 96.4 ± 1.9, $p > 0.05$, $n = 12$). These results indicate that DPI significantly attenuates $Ca^{2+}$ release from the SR on depolarization in ventricular myocytes, and that such reduction in $Ca^{2+}$ release may be associated with the decrease in SR $Ca^{2+}$ loading.

## Suppression of $I_{Ca}$ by DPI

The $Ca^{2+}$ release in cardiac myocytes on depolarization is

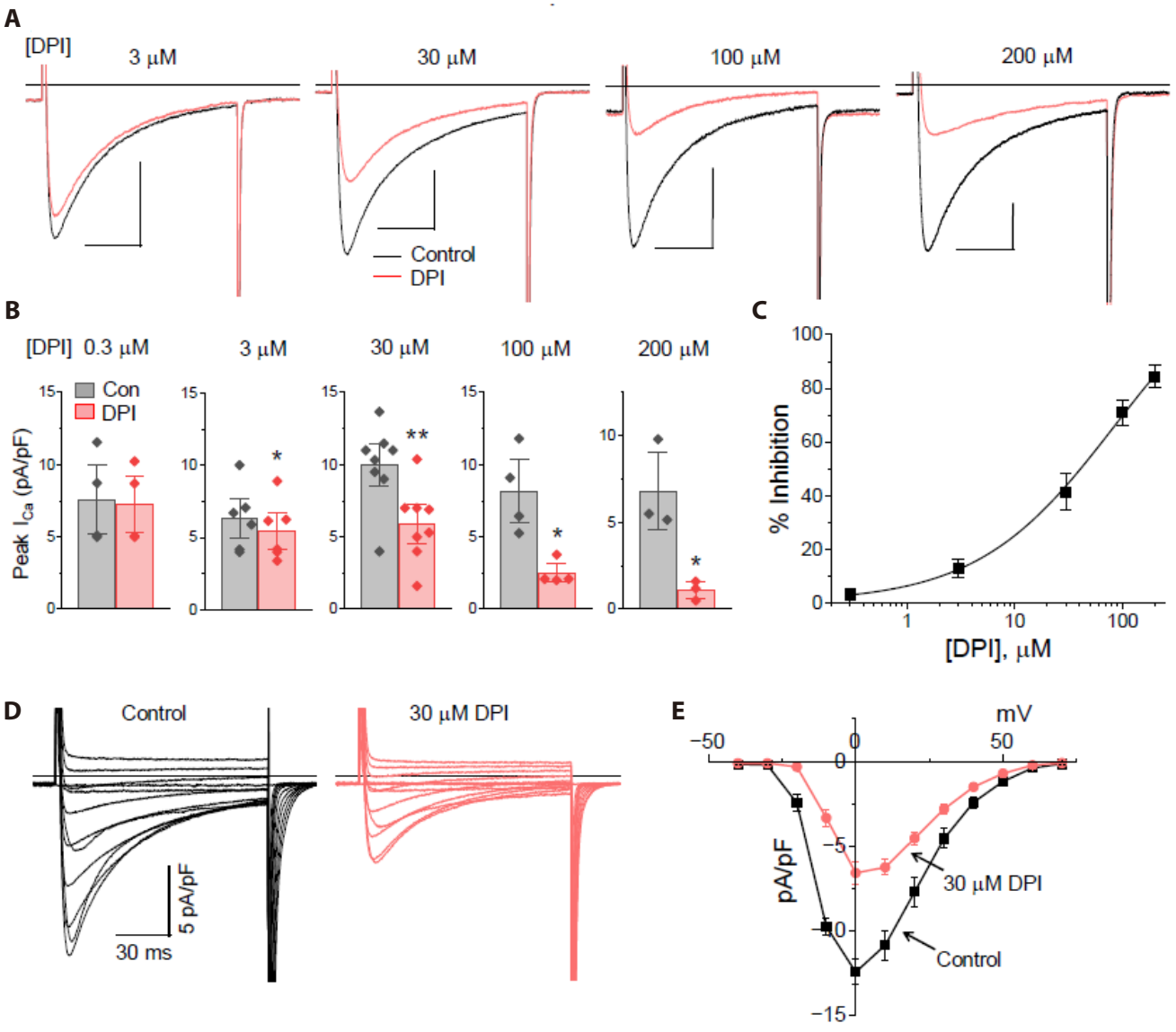


**Fig. 3. Suppression of $Ca^{2+}$ current ($I_{Ca}$) by diphenyleneiodonium (DPI).** (A) Superimposed $I_{Ca}$ recorded at 0 mV (holding potential at –40 mV) before and after applications of 3 μM, 30 μM, 100 μM, and 200 μM DPI in the representative ventricular myocytes, showing concentration-dependent inhibition in $I_{Ca}$ by DPI. Scale bars indicate 30 ms in x axis and 2 pA/pF in y axis. (B) Comparison of mean peak $I_{Ca}$ measured under control conditions and after applications of different concentrations of DPI (0.3 μM, $n = 3$; 3 μM, $n = 6$; 30 μM, $n = 8$; 100 μM, $n = 4$; 200 μM, $n = 3$). **$p < 0.01$, *$p < 0.05$ *vs.* control (Con). Paired t-test. (C) Concentration-dependence curve for % inhibition in $I_{Ca}$ *versus* concentrations of DPI. Plot was fit with Hill equation (Hill coefficient = 0.68). (D) Superimposed $I_{Ca}$ measured at voltage steps ranging –40 to +70 mV (holding at –40 mV) with 10-mV-increment before (Control) and after application of 30 μM DPI in a representative ventricle cell. (E) Current-voltage relationships of averaged $I_{Ca}$ at the step potentials in the control condition and after exposure to 30 μM DPI ($n = 3$). Cells were dialyzed with 15 mM EGTA containing internal solutions.

mainly controlled by $Ca^{2+}$ influx through the L-type $Ca^{2+}$ channels [1-4]. $I_{Ca}$ also contributes to loading of $Ca^{2+}$ into the SR. To understand the cellular mechanism for DPI-induced reductions in $Ca^{2+}$ transient and SR $Ca^{2+}$ content (Fig. 2), we next tested whether DPI alters $I_{Ca}$. The effects of different concentrations of DPI (0.3–200 μM) on $I_{Ca}$ were tested using whole-cell patch clamp technique (see METHODS). The $I_{Ca}$ was continuously measured at 0.1 Hz during a voltage step to 0 mV from a holding potential of –40 mV. There was no change in $I_{Ca}$ in the presence of 0.3 μM (Fig. 3B). The application of DPI at 3 μM slightly but significantly reduced the peak $I_{Ca}$ (Fig. 3; by 12 ± 3.3%, $n$ = 6, $p < 0.05$). This effect by DPI was not mimicked by the application of the specific inhibitors of Nox 2 and Nox 4—the most abundantly expressed isoforms of Nox in adult cardiac myocytes [32] (Supplementary Fig. 1). Higher concentrations of DPI suppressed $I_{Ca}$ more strongly in a concentration-dependent manner with $IC_{50}$ value of ≅40 μM (Fig. 3A–C; 30 μM: 41 ± 6.9%, $n$ = 8, $p < 0.01$; 100 μM, 71 ± 4.7, $n$ = 4, $p < 0.05$; 200 μM, 84 ± 4.1%, $n$ = 3, $p < 0.05$). The time constant of inactivation of $I_{Ca}$, measured with curve fitting (see METHODS), was slightly increased by the application of 30 μM DPI (control, 24.4 ± 1.35 ms; 30 μM DPI, 27.8 ± 1.62 ms, $p < 0.05$, $n$ = 9). We measured the current-voltage relationship of the $I_{Ca}$ before and after application of submaximal concentrations of DPI (30 μM), and found there was no significant change in the current-voltage relationship by DPI (Fig. 3D, E). These results suggest that the attenuations of $Ca^{2+}$ transients and SR $Ca^{2+}$ loading in the presence of 3 μM DPI may be caused by $I_{Ca}$ suppression. The concentration-dependent inhibition of contractility in the presence of DPI is also consistent with stronger suppression in $I_{Ca}$ by the higher concentrations of DPI.

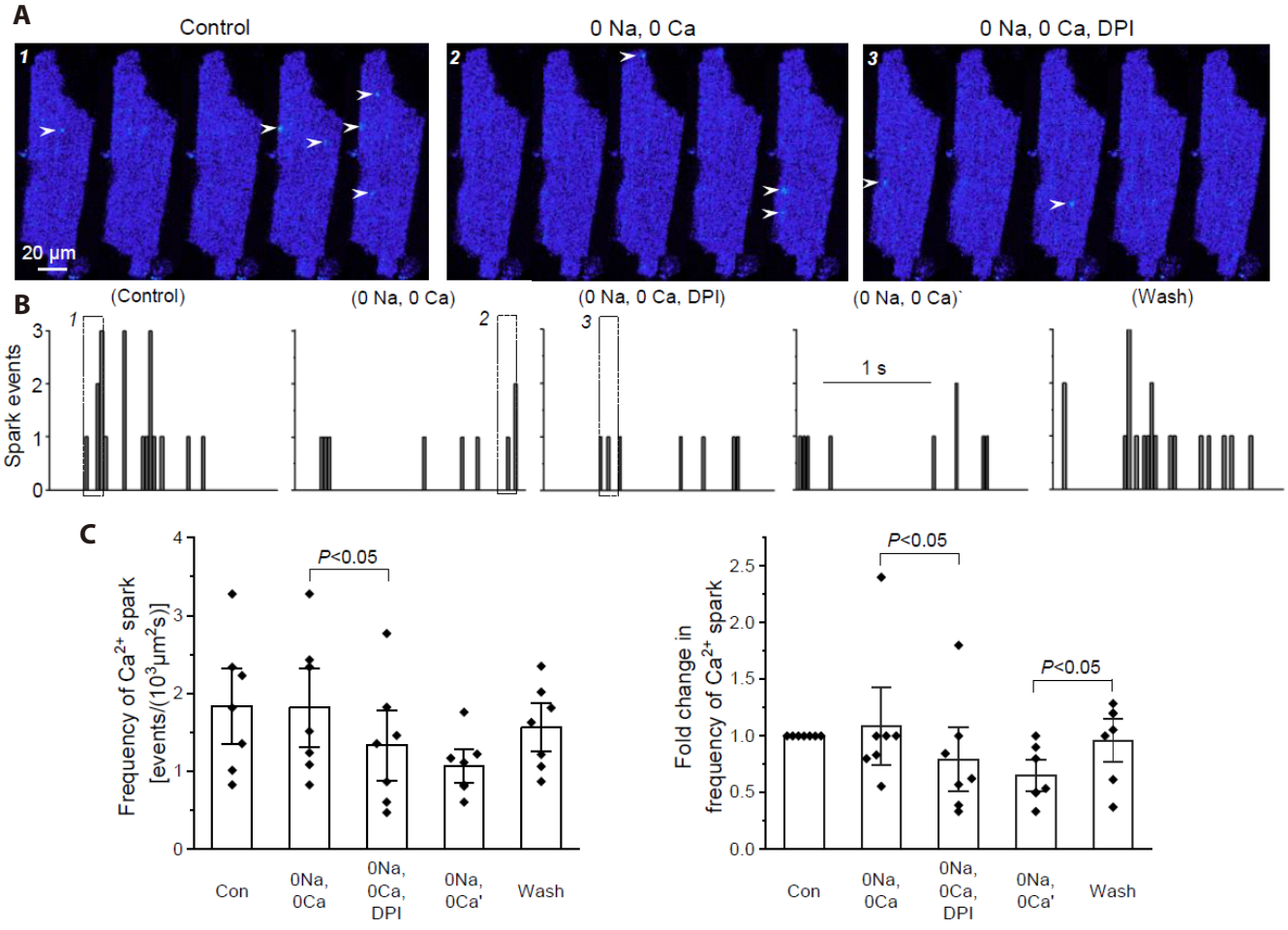


**Fig. 4. Suppression of $Ca^{2+}$ sparks by diphenyleneiodonium (DPI) in the absence of external $Na^+$ and $Ca^{2+}$.** (A) A series of sequential confocal $Ca^{2+}$ images recorded at 30 Hz from a representative resting rat ventricular myocyte in the control condition ("1") and after brief exposure to zero $Na^+$ and zero $Ca^{2+}$ external solutions (0 Na, 0 Ca) for 10 s ("2"), followed by additional application of DPI (0 Na, 0 Ca, DPI) for 3 min ("3"). The images were selected from the periods marked with the boxes correspondingly numbered ("1", "2", and "3") in the panel B. After 3-min DPI application, DPI was removed from the zero $Na^+$ and zero $Ca^{2+}$ solutions (2 min; (0 Na, 0 Ca, DPI)`), which was followed by the exchange of external solution with control solutions (5 min; "Wash"). Arrows indicate distinct $Ca^{2+}$ sparks. (B) Plots of the total numbers of sparks occurred in each frame (33 frames/s) *versus* 2-s-long recording periods under each condition labeled above the plots. (C) Summary of mean spark frequency detected under each condition indicated underneath the graphs. Paired t-test was used.

### DPI-induced suppression of $Ca^{2+}$ sparks independently of external $Na^+$- and $Ca^{2+}$-flux

We have previously observed that DPI at the concentrations of 3 μM decreased the frequency of spontaneous $Ca^{2+}$ sparks in rat ventricular myocytes [18]. Since the $Ca^{2+}$ sparks represent elementary $Ca^{2+}$ releases through the RyR clusters composing global $Ca^{2+}$ increase during $I_{Ca}$ in cardiac myocytes [5-9], one of possible mechanisms for decrease in global $Ca^{2+}$ releases on depolarization in the presence of DPI is such reduction in the activity of RyRs. We further examined whether external $Ca^{2+}$- and/or $Na^+$-mediated ionic flux through the cell membrane plays a role in suppression of $Ca^{2+}$ releases in the cells treated with DPI, we tested the effects of removal of external $Na^+$ and $Ca^{2+}$ on DPI-induced $Ca^{2+}$ spark suppression.

To quantify the occurrence of $Ca^{2+}$ sparks, we performed 2 s-long 2-D confocal $Ca^{2+}$ imaging at 30 Hz to monitor a major part of the ventricular cells. Conditioning electrical stimulations were applied to stabilize SR $Ca^{2+}$ loading before measuring spontaneous $Ca^{2+}$ sparks. Under this control conditions, $Ca^{2+}$ sparks spontaneously occurred at a frequency of 1.82 ± 0.23 events/$10^3$ $\mu m^2$·s ($n$ = 11). The treatment of 3 μM DPI suppressed the spark frequency to 1.17 ± 0.17 events/$10^3$ $\mu m^2$·s ($n$ = 11) within 2–3-min of treatment ($p < 0.01$), consistent with the previous report [18]. When the external $Na^+$ and $Ca^{2+}$ were shortly removed (see METHODS), the spark frequency was not significantly changed (control, 1.83 ± 0.32 *vs.* zero $Na^+$ and $Ca^{2+}$, 1.81 ± 0.33, $p > 0.05$, $n$ = 7). In the continued presence of external zero $Na^+$ and zero $Ca^{2+}$ solutions, application of DPI still reduced the spark frequency by ~25% (DPI in zero $Na^+$ and $Ca^{2+}$: 1.34 ± 0.30, $p < 0.05$, $n$ = 7) (Fig. 4). This result suggests that other $Ca^{2+}$ entry and $Ca^{2+}$- and/or $Na^+$-dependent membrane ionic flux may not contribute to suppression of spontaneous $Ca^{2+}$ sparks in the presence of DPI.

### Decrease in mitochondrial ROS level by DPI

A line of previous reports indicate that long-term injection of DPI can cause mitochondrial myopathy in animal models by impairing oxidative phosphorylation, particularly Complex 1 activity [22-25]. Complex I is essential for ATP synthesis and can generate ROS in the cardiac muscle mitochondria. Inhibition of Complex 1 by DPI has reduced mitochondrial $O_2^{\cdot-}$ in unstimulated monocyte/macrophage [33] and in isolated mitochondria from guinea-pig cardiac myocytes [34]. Oxidation of the thiol groups in RyR2 by ROS enhances its channel activity, whereas their reduction inhibits the channels [35-37]. Therefore, in the next series of experiments, we tested whether DPI also affects mitochondrial ROS level in rat ventricular myocytes under control conditions using confocal imaging with MitoSOX-red, the mitochondrial $O_2^{\cdot-}$ indicator. We found that application of DPI at 3–100 μM elicited significant decreases in the mitochondrial $O_2^{\cdot-}$ level in these myocytes (Fig. 5). These results support the notion that reduction in spontaneous spark frequency in the presence of 3 μM DPI with no external $Ca^{2+}$ and $Na^+$ (Fig. 4) may be due to decrease in mitochondrial ROS level.

## DISCUSSION

In this study, we demonstrate for the first time that DPI exerts negative inotropic effects on cardiac myocytes (Fig. 1), and that such negative inotropy can be mediated by the suppression of $I_{Ca}$ and $Ca^{2+}$-induced $Ca^{2+}$ release upon depolarization (Figs. 2 and 3). The suppressive effect on $I_{Ca}$ by DPI was not mimicked by other specific Nox inhibitors (Supplementary Fig. 1). We also showed that this chemical significantly reduces SR $Ca^{2+}$ loading and the occurrence of $Ca^{2+}$ sparks at the concentrations (3 μM) used to investigate the role of Nox in mammalian cells including cardiac myocytes (Figs. 2 and 4). The suppression of resting $Ca^{2+}$ spark occurrence by DPI was not altered when the external $Ca^{2+}$

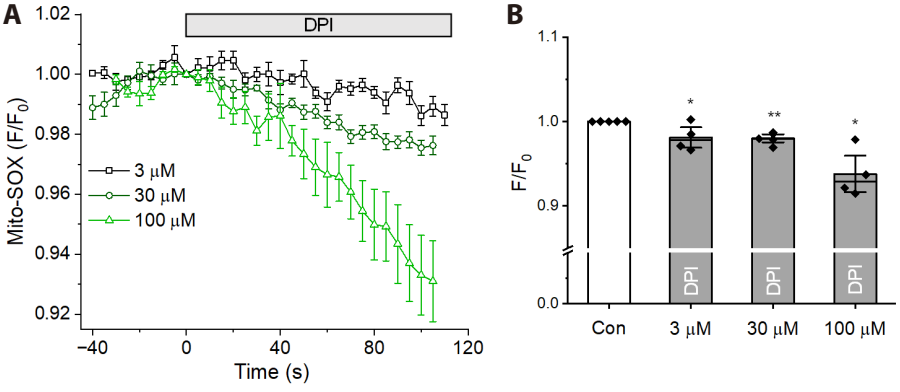


**Fig. 5. Reduction of mitochondrial superoxide by diphenyleneiodonium (DPI).** (A) Plots of averaged Mito-SOX fluorescence, normalized to the levels ($F_0$) just prior to the application of DPI (3 μM, $n$ = 4; 30 μM, $n$ = 5; 100 μM, $n$ = 4), *versus* recording time, showing decrease of mitochondrial superoxide levels by DPI in a concentration-dependent manner. (B) Summary of Mito-SOX fluorescence ratio measured at 100-s after the onset of DPI applications, showing DPI-induced signal reductions at 3 μM, 30 μM, and 100 μM DPI. **$p < 0.01$, *$p < 0.05$ *vs.* control (Con) (paired t-test).

and $Na^+$ were removed (Fig. 4), suggesting that $I_{Ca}$-independent mechanism may be involved in spark suppression by DPI. Mitochondrial superoxide level was significantly reduced by DPI at the concentration of 3–100 μM. These results indicate that DPI suppresses $Ca^{2+}$ channels and RyRs, thereby eliciting negative inotropy in cardiac myocytes, and suggest that the effects of DPI may involve its inhibitory action on mitochondrial metabolism independently of Nox.

Decreases in the $I_{Ca}$ and SR $Ca^{2+}$ loading can underlie decreases in the $Ca^{2+}$ transient magnitudes in cells exposed to DPI (Figs. 2 and 3). However, the decrease in the $Ca^{2+}$ transients may partly explain the negative inotropy of ventricular myocytes during the DPI exposure. At the concentrations of 3 μM, the magnitude of $Ca^{2+}$ transients were reduced by approximately 20% (Fig. 2A, B), while cell shortenings were decreased by 50%–60% (Fig. 1). In addition, at the concentrations of 0.3 μM, contraction was significantly decreased by DPI (Fig. 1), although $I_{Ca}$ was not altered (Fig. 3). These results suggest that other mechanisms may be involved in the negative inotropy by DPI. In this regard, it has been reported in skeletal muscle that DPI causes fatigue and force failure *via* irreversible impairment in oxidative phosphorylation, particularly Complex 1 activity [22-25]. Potent and strong inhibition in contraction by DPI may be caused by such reduction in ATP production by mitochondria.

Reduction in SR $Ca^{2+}$ loading in the presence of DPI could be a result of decreased $Ca^{2+}$ influx through the $Ca^{2+}$ channels (Figs. 2D and 3). Because most of the $Ca^{2+}$ removal during the decay phase of $Ca^{2+}$ transient is thought to be mediated by SR $Ca^{2+}$ pump in ventricular myocytes from *rat* heart [38], one can indirectly approximate the activity of SR $Ca^{2+}$ pump with evaluating the speed of $Ca^{2+}$ transient decay. No change in the half decay time of $Ca^{2+}$ transient in the presence of 3 μM DPI (Fig. 2C) suggests that the decrease in SR $Ca^{2+}$ content by DPI may not be caused by alteration in the activity of SR $Ca^{2+}$ pump. Nevertheless, it should also be noted, in the microsome preparation from pig coronary artery, that DPI at the concentrations of > 10 μM has exerted mild inhibitory effects on SR $Ca^{2+}$ pump activity [26].

Resting $Ca^{2+}$ spark frequency was reduced by 3 μM DPI even in the absence of external $Na^+$ and $Ca^{2+}$ (Fig. 4), suggesting suppression of *in situ* activity of RyR2 clusters in cardiac myocytes exposed to this chemical regardless of $I_{Ca}$ and/or $Na^+$–$Ca^{2+}$ exchanger. We have previously found that suppressive effect by DPI on the spark frequency is not mimicked by the application of inhibitor for either Nox 2 (gp91-ds) or NOS (L-NAME) in rat ventricular myocytes [18]. In addition, inhibition of xanthine oxidase, one of the ROS producing enzymes that is sensitive to DPI [29], has rather enhanced ventricular sparks in rats [39], which excludes its role in the effect of DPI on $Ca^{2+}$ sparks. It is plausible to suggest that the suppressive effect by DPI on the resting spark frequency could be indirectly caused by decrease in SR $Ca^{2+}$ content (Fig. 2), since SR luminal $Ca^{2+}$ plays a role in sensitizing RyR to $Ca^{2+}$ in cardiac myocytes [40,41]. Nevertheless, reversible and quick effects of DPI on the spark frequency (Fig. 4) may reflect other mechanism involved in modulation of RyRs by DPI, such as reduction of thiol groups on RyR by decrease of mitochondrial ROS level in the vicinity [11,35-37]. Since we observed mitochondrial ROS reduction during application of DPI at similar concentrations of DPI (Fig. 5), such notion may be possible.

Nox 2 and Nox 4 are the most abundant Nox isoforms in cardiac myocytes [32]. The former is a key signaling protein to generate ROS in the transverse-tubules of cardiac myocytes under external or mechanical stress [16,17] and the latter has been thought to play a role in mitochondrial ROS generation under pathological conditions, such as cardiomyopathy and hypertrophy [32,42]. Nox generates $O_2^{\cdot-}$ in a highly regulated manner with a stimulus dependent cell-signaling pathways unlike other ROS sources, such as xanthin oxidase and mitochondrial respiratory chain [14-19]. Although current experiments were performed in the control conditions with no stress, possibility that Nox inhibition contributes to DPI-induced mitochondrial ROS reduction in normal cardiac myocytes under control conditions may not be completely excluded. Inhibition of Complex I in the mitochondrial respiratory chain by DPI [22-25] has been shown to decrease cellular and mitochondrial ROS in macrophages and in isolated mitochondria from guinea-pig cardiac myocytes [33,34]. These reports seem to be consistent with our observation on DPI-induced ROS reduction in the mitochondria of rat ventricular myocytes (Fig. 5). It should be noted, however, that increase in ROS level by DPI has also been reported in other cell type and/or experimental conditions [43].

Slight but significant suppression in $I_{Ca}$ in the presence of 3 μM DPI was not mimicked by other specific Nox inhibitors, such as the Nox-2-blocking peptide gp91ds-tat and the Nox-4-specific inhibitor setanaxib (Supplementary Fig. 1). In addition, inhibition of NOS using L-NAME did not significantly alter $I_{Ca}$ in these myocytes (Supplementary Fig. 2). These support that Nox and NOS are not involved in the suppressive effect by DPI on $I_{Ca}$ in cardiac myocytes under control conditions. The effect of DPI on membrane ion channels including $Ca^{2+}$ channels have been recognized previously at the similar concentrations in other cell types, for examples, neuron from carotid body and smooth muscle cells of pulmonary vasculature [44,45]. The mechanism for DPI-induced $I_{Ca}$ suppression, however, has not been fully understood. In this regard, it has been shown that an addition of $H_2O_2$ in the presence of DPI has not reversed the inhibitory effect by DPI on $I_{Ca}$ in pulmonary smooth muscle cells [44]. Molecular mechanism for the $I_{Ca}$ suppression by DPI *via* the mitochondrial inhibition (*e.g.*, Complex I) remains uncertain. Further studies will be required to determine whether the mechanisms including 1) attenuated mitochondrial $Ca^{2+}$ uptake to inactivate $I_{Ca}$ [46], 2) a drop of cytosolic pH [47] resulting from suppression of oxidative phosphorylation (increased anaerobic glycolysis), or 3) loss of ATP and/or $Ca^{2+}$-dependent channel phosphorylation by kinases [48] such as CaMKII or PKC, play a role in the inhibition of $I_{Ca}$ by DPI.

Strong suppressions in $I_{Ca}$ and contraction at high concentrations of DPI appear to elicit cardiac toxicity. Such DPI effects appear to be similar to the $H_2S$- or rotenone-mediated toxicity in cardiac myocytes in terms of the modulations of contraction and mitochondrial metabolism [49,50]. Interestingly, $H_2S$- or rotenone-mediated cardiotoxicity was reversed by the application of methylene blue [50]. It would be worth investigating the effects of DPI in combination with methylene blue, $H_2S$ and/or rotenone to further delineate the mode of action of DPI in the modulation of cardiac excitation-contraction coupling.

DPI induces negative inotropy in cardiac myocytes and attenuate $Ca^{2+}$-induced $Ca^{2+}$ releases *via* suppression of L-type $Ca^{2+}$ channel, SR $Ca^{2+}$ loading and RyRs in the presence of popular concentrations of DPI used to inhibit Nox. In addition, the results suggest that ventricular contractile machinery is more sensitive to DPI compared to $Ca^{2+}$ channels. Its effects on $I_{Ca}$ and RyRs appear to be independent of inhibition of Nox or NOS. Since DPI significantly reduced ROS in the mitochondria the suppression of RyRs by such ROS decrease is likely. Since $Ca^{2+}$ is a ubiquitous signaling molecule, DPI-induced secondary effects on other proteins are expected. This raises needs for a caution to interpret experimental results collected with the use of DPI. In this regard, our data obtained in cardiac $Ca^{2+}$ signaling and contraction may help dissecting a role of Nox itself in cardiac functional regulation under various environments.

## FUNDING

The work was supported by National Research Foundation of Korea (NRF) grants funded by the Korea government (2022R1A2C209158311 and 2022R1A5A708515611).

## ACKNOWLEDGEMENTS

None.

## CONFLICTS OF INTEREST

The authors declare no conflicts of interest.

## SUPPLEMENTARY MATERIALS

Supplementary data including two figures can be found with this article online at https://doi.org/10.4196/kjpp.2024.28.4.335

## REFERENCES

1. Fabiato A. Calcium-induced release of calcium from the cardiac sarcoplasmic reticulum. *Am J Physiol*. 1983;245:C1-C14.
2. Beuckelmann DJ, Wier WG. Mechanism of release of calcium from sarcoplasmic reticulum of guinea-pig cardiac cells. *J Physiol*. 1988;405:233-255.
3. Näbauer M, Callewaert G, Cleemann L, Morad M. Regulation of calcium release is gated by calcium current, not gating charge, in cardiac myocytes. *Science*. 1989;244:800-803.
4. Niggli E, Lederer WJ. Voltage-independent calcium release in heart muscle. *Science*. 1990;250:565-568.
5. Cheng H, Lederer WJ, Cannell MB. Calcium sparks: elementary events underlying excitation-contraction coupling in heart muscle. *Science*. 1993;262:740-744.
6. Cannell MB, Cheng H, Lederer WJ. Spatial non-uniformities in $[Ca^{2+}]_i$ during excitation-contraction coupling in cardiac myocytes. *Biophys J*. 1994;67:1942-1956.
7. Wier WG, Egan TM, López-López JR, Balke CW. Local control of excitation-contraction coupling in rat heart cells. *J Physiol*. 1994;474:463-471.
8. Shacklock PS, Wier WG, Balke CW. Local $Ca^{2+}$ transients ($Ca^{2+}$ sparks) originate at transverse tubules in rat heart cells. *J Physiol*. 1995;487:601-608.
9. Parker I, Zang WJ, Wier WG. $Ca^{2+}$ sparks involving multiple $Ca^{2+}$ release sites along Z-lines in rat heart cells. *J Physiol*. 1996;497:31-38.
10. Zima AV, Blatter LA. Redox regulation of cardiac calcium channels and transporters. *Cardiovasc Res*. 2006;71:310-321.
11. Yan Y, Liu J, Wei C, Li K, Xie W, Wang Y, Cheng H. Bidirectional regulation of $Ca^{2+}$ sparks by mitochondria-derived reactive oxygen species in cardiac myocytes. *Cardiovasc Res*. 2008;77:432-441.
12. Terentyev D, Györke I, Belevych AE, Terentyeva R, Sridhar A, Nishijima Y, de Blanco EC, Khanna S, Sen CK, Cardounel AJ, Carnes CA, Györke S. Redox modification of ryanodine receptors contributes to sarcoplasmic reticulum $Ca^{2+}$ leak in chronic heart failure. *Circ Res*. 2008;103:1466-1472.
13. Cooper LL, Li W, Lu Y, Centracchio J, Terentyeva R, Koren G, Terentyev D. Redox modification of ryanodine receptors by mitochondria-derived reactive oxygen species contributes to aberrant $Ca^{2+}$ handling in ageing rabbit hearts. *J Physiol*. 2013;591:5895-5911.
14. Bedard K, Krause KH. The NOX family of ROS-generating NADPH oxidases: physiology and pathophysiology. *Physiol Rev*. 2007;87:245-313.
15. Akki A, Zhang M, Murdoch C, Brewer A, Shah AM. NADPH oxidase signaling and cardiac myocyte function. *J Mol Cell Cardiol*. 2009;47:15-22.
16. Prosser BL, Ward CW, Lederer WJ. X-ROS signaling: rapid mecha-no-chemo transduction in heart. *Science*. 2011;333:1440-1445.
17. Jian Z, Han H, Zhang T, Puglisi J, Izu LT, Shaw JA, Onofiok E, Erickson JR, Chen YJ, Horvath B, Shimkunas R, Xiao W, Li Y, Pan T, Chan J, Banyasz T, Tardiff JC, Chiamvimonvat N, Bers DM, Lam KS, *et al*. Mechanochemotransduction during cardiomyocyte contraction is mediated by localized nitric oxide signaling. *Sci Signal*. 2014;7:ra27.
18. Kim JC, Wang J, Son MJ, Woo SH. Shear stress enhances $Ca^{2+}$ sparks through Nox2-dependent mitochondrial reactive oxygen species generation in rat ventricular myocytes. *Biochim Biophys*

*Acta Mol Cell Res*. 2017;1864:1121-1131.
19. Looi YH, Grieve DJ, Siva A, Walker SJ, Anilkumar N, Cave AC, Marber M, Monaghan MJ, Shah AM. Involvement of Nox2 NADPH oxidase in adverse cardiac remodeling after myocardial infarction. *Hypertension*. 2008;51:319-325.
20. Cross AR, Jones OT. The effect of the inhibitor diphenylene iodonium on the superoxide-generating system of neutrophils. Specific labelling of a component polypeptide of the oxidase. *Biochem J*. 1986;237:111-116.
21. Zhang M, Perino A, Ghigo A, Hirsch E, Shah AM. NADPH oxidases in heart failure: poachers or gamekeepers? *Antioxid Redox Signal*. 2013;18:1024-1041.
22. Bloxham DP. The relationship of diphenyleneiodonium-induced hypoglycaemia to the specific covalent modification of NADH-ubiquinone oxidoreductase. *Biochem Soc Trans*. 1979;7:103-106.
23. Cooper JM, Petty RK, Hayes DJ, Morgan-Hughes JA, Clark JB. Chronic administration of the oral hypoglycaemic agent diphenyleneiodonium to rats. An animal model of impaired oxidative phosphorylation (mitochondrial myopathy). *Biochem Pharmacol*. 1988;37:687-694.
24. Majander A, Finel M, Wikström M. Diphenyleneiodonium inhibits reduction of iron-sulfur clusters in the mitochondrial NADH-ubiquinone oxidoreductase (Complex I). *J Biol Chem*. 1994;269:21037-21042.
25. Paradies G, Petrosillo G, Pistolese M, Di Venosa N, Federici A, Ruggiero FM. Decrease in mitochondrial complex I activity in ischemic/reperfused rat heart: involvement of reactive oxygen species and cardiolipin. *Circ Res*. 2004;94:53-59.
26. Tazzeo T, Worek F, Janssen Lj. The NADPH oxidase inhibitor diphenyleneiodonium is also a potent inhibitor of cholinesterases and the internal Ca$^{(2+)}$ pump. *Br J Pharmacol*. 2009;158:790-796.
27. Stuehr DJ, Fasehun OA, Kwon NS, Gross SS, Gonzalez JA, Levi R, Nathan CF. Inhibition of macrophage and endothelial cell nitric oxide synthase by diphenyleneiodonium and its analogs. *FASEB J*. 1991;5:98-103.
28. Dodd-o JM, Zheng G, Silverman HS, Lakatta EG, Ziegelstein RC. Endothelium-independent relaxation of aortic rings by the nitric oxide synthase inhibitor diphenyleneiodonium. *Br J Pharmacol*. 1997;120:857-864.
29. Sanders SA, Eisenthal R, Harrison R. NADH oxidase activity of human xanthine oxidoreductase--generation of superoxide anion. *Eur J Biochem*. 1997;245:541-548.
30. Wang J, Trinh TN, Vu ATV, Kim JC, Hoang ATN, Ohk CJ, Zhang YH, Nguyen CM, Woo SH. Chrysosplenol-C increases contraction by augmentation of sarcoplasmic reticulum $Ca^{2+}$ loading and release via protein kinase C in rat ventricular myocytes. *Mol Pharmacol*. 2022;101:13-23.
31. Lee S, Kim JC, Li Y, Son MJ, Woo SH. Fluid pressure modulates L-type $Ca^{2+}$ channel via enhancement of $Ca^{2+}$-induced $Ca^{2+}$ release in rat ventricular myocytes. *Am J Physiol Cell Physiol*. 2008;294:C966-C976.
32. Byrne JA, Grieve DJ, Bendall JK, Li JM, Gove C, Lambeth JD, Cave AC, Shah AM. Contrasting roles of NADPH oxidase isoforms in pressure-overload versus angiotensin II-induced cardiac hypertrophy. *Circ Res*. 2003;93:802-805.
33. Li Y, Trush MA. Diphenyleneiodonium, an NAD(P)H oxidase inhibitor, also potently inhibits mitochondrial reactive oxygen species production. *Biochem Biophys Res Commun*. 1998;253:295-299.
34. Hool LC, Di Maria CA, Viola HM, Arthur PG. Role of NAD(P)H oxidase in the regulation of cardiac L-type $Ca^{2+}$ channel function during acute hypoxia. *Cardiovasc Res*. 2005;67:624-635.
35. Trimm JL, Salama G, Abramson JJ. Sulfhydryl oxidation induces rapid calcium release from sarcoplasmic reticulum vesicles. *J Biol Chem*. 1986;261:16092-16098.
36. Boraso A, Williams AJ. Modification of the gating of the cardiac sarcoplasmic reticulum Ca$^{(2+)}$-release channel by $H_2O_2$ and dithiothreitol. *Am J Physiol*. 1994;267:H1010-H1016.
37. Marengo JJ, Hidalgo C, Bull R. Sulfhydryl oxidation modifies the calcium dependence of ryanodine-sensitive calcium channels of excitable cells. *Biophys J*. 1998;74:1263-1277.
38. Bers DM. Cardiac excitation-contraction coupling. *Nature*. 2002;415:198-205.
39. Zima AV, Copello JA, Blatter LA. Effects of cytosolic NADH/NAD(+) levels on sarcoplasmic reticulum Ca$^{(2+)}$ release in permeabilized rat ventricular myocytes. *J Physiol*. 2004;555:727-741.
40. Györke S, Lukyanenko V, Györke I. Dual effects of tetracaine on spontaneous calcium release in rat ventricular myocytes. *J Physiol*. 1997;500:297-309.
41. Satoh H, Blatter LA, Bers DM. Effects of $[Ca^{2+}]_i$, SR $Ca^{2+}$ load, and rest on $Ca^{2+}$ spark frequency in ventricular myocytes. *Am J Physiol*. 1997;272:H657-H668.
42. Vendrov AE, Xiao H, Lozhkin A, Hayami T, Hu G, Brody MJ, Sadoshima J, Zhang YY, Runge MS, Madamanchi NR. Cardiomyocyte NOX4 regulates resident macrophage-mediated inflammation and diastolic dysfunction in stress cardiomyopathy. *Redox Biol*. 2023;67:102937.
43. Rana M, Setia M, Suvas PK, Chakraborty A, Suvas S. Diphenyleneiodonium treatment inhibits the development of severe herpes stromal keratitis lesions. *J Virol*. 2022;96:e0101422.
44. Weir EK, Wyatt CN, Reeve HL, Huang J, Archer SL, Peers C. Diphenyleneiodonium inhibits both potassium and calcium currents in isolated pulmonary artery smooth muscle cells. *J Appl Physiol*. 1994;76:2611-2615.
45. Wyatt CN, Weir EK, Peers C. Diphenylene iodonium blocks $K^+$ and $Ca^{2+}$ currents in type I cells isolated from the neonatal rat carotid body. *Neurosci Lett*. 1994;172:63-66.
46. Sánchez JA, García MC, Sharma VK, Young KC, Matlib MA, Sheu SS. Mitochondria regulate inactivation of L-type $Ca^{2+}$ channels in rat heart. *J Physiol*. 2001;536.2:387-396.
47. Irisawa H, Sato R. Intra- and extracellular actions of proton on the calcium current of isolated guinea pig ventricular cells. *Circ Res*. 1986;59:48-355.
48. Chantawansri C, Huynh N, Yamanaka J, Garfinkel A, Lamp ST, Inoue M, Bridge JH, Goldhaber JI. Effect of metabolic inhibition on couplon behavior in rabbit ventricular myocytes. *Biophys J*. 2008;94:1656-1666.
49. Haouzi P, Sonobe T, Judenherc-Haouzi A. Developing effective countermeasures against acute hydrogen sulfide intoxication: challenges and limitations. *Ann N Y Acad Sci*. 2016;1374:29-40.
50. Cheung JY, Wang J, Zhang XQ, Song J, Davidyock JM, Prado FJ, Shanmughapriya S, Worth AM, Madesh M, Judenherc-Haouzi A, Haouzi P. Methylene blue counteracts $H_2S$-induced cardiac ion channel dysfunction and ATP reduction. *Cardiovasc Toxicol*. 2018;18:407-419.